

# Optical Coherence Tomography of the Tympanic Membrane and Middle Ear: A Review

Hsern Ern Ivan Tan, MBBS (1,2,3)

Peter Luke Santa Maria, MBBS, PhD (1,2,4)

Philip Wijesinghe, PhD (5,6)

Brendan Kennedy, PhD (5,6)

Benjamin James Allardyce, PhD (7)

Robert Henry Eikelboom, PhD (1,2,8)

Marcus David Atlas, MBBS (1,2)

Rodney James Dilley, PhD (1,2)

## Affiliations

1. Ear Science Institute Australia, Subiaco, Australia
2. Ear Sciences Centre, School of Medicine, The University of Western Australia, Nedlands, Australia
3. Department of Otolaryngology, Head and Neck Surgery, Sir Charles Gairdner Hospital, Perth, Western Australia
4. Department of Otolaryngology, Head and Neck Surgery, Stanford University, California, USA
5. BRITELab, Harry Perkins Institute of Medical Research, QEII Medical Centre, Nedlands and Centre for Medical Research, The University of Western Australia, Nedlands, Australia.
6. Department of Electrical, Electronic and Computer Engineering, The University of Western Australia, Nedlands, Australia
7. Deakin University, Institute for Frontier Materials, Geelong, Australia
8. Department of Speech Language Pathology and Audiology, University of Pretoria, Pretoria, South Africa

## Corresponding Author's Institution

Ear Science Institute Australia, Subiaco, Australia

## Financial Disclosures

None

### Conflict of Interest

BK is a Founder of, has equity and receives research support from OncoRes Medical developing optical coherence elastography for surgical applications. No other authors declare any relevant financial disclosures.

### Author Correspondence

Name: Dr Hsern Ern Tan

Address: Ear Science Institute Australia, SNRI Building, QE II Medical Centre, Level 3, 8 Verdun Street, Nedlands WA 6009

Email: hsern.ern.tan@earsience.org.au

Phone No: +61 421 162 715

### Presentations

This work was presented at the ARO 41<sup>st</sup> Annual MidWinter Meeting 2018 held in San Diego, CA.

### Keywords

Tympanic membrane, optical coherence tomography, imaging

# Abstract

## Objective:

To evaluate the recent developments in optical coherence tomography (OCT) for tympanic membrane (TM) and middle ear (ME) imaging, and to identify what further development is required for the technology to be integrated into common clinical use.

## Data Sources:

PubMed, Embase, Google Scholar, Scopus and Web of Science.

## Review Methods:

A comprehensive literature search for English language articles published from January 1966 to January 2018 with the keywords “tympanic membrane or middle ear”, “optical coherence tomography” and “imaging” was performed.

## Conclusion:

Conventional imaging techniques cannot adequately resolve the microscale features of TM and ME, sometimes necessitating diagnostic exploratory surgery in challenging otological pathology. As a high-resolution, non-invasive imaging technique, OCT offers promise as a diagnostic aid for otologic conditions such as otitis media, cholesteatoma and conductive hearing loss. Using OCT vibrometry to image the nanoscale vibrations of the TM and ME as they conduct acoustic waves may detect the location of ossicular chain dysfunction, and differentiate between stapes fixation and incus-stapes discontinuity. The capacity of OCT to image depth and thickness at high-resolution allows 3D-volumetric reconstruction of the ME and has potential use for reconstructive tympanoplasty planning and the follow-up of ossicular prostheses.

## Implications for Practice:

To achieve common clinical use beyond these initial discoveries, future in-vivo imaging devices must feature low-cost probe or endoscopic designs, faster imaging speeds and demonstrate superior diagnostic utility to CT and MRI. While such technology has been available for OCT, its translation requires focused development through a close collaboration between engineers and clinicians.

# Introduction

The traditional otoscope and surgical microscope are essential visualisation tools for the otolaryngologist, long serving as the premier diagnostic and operative tools for otological pathology. However, as the optical design of these instruments only allows for the magnification and illumination of the tympanic membrane (TM), there are several weaknesses. Otoscopy can only provide visualisation of the lateral surface of the TM, through the narrow field of view afforded by the ear canal and unless utilising an oto-endoscope, the full surface of the TM cannot usually be seen in one view. The view is also only two-dimensional, resulting in a subjective interpretation of the three-dimensional TM shape. Furthermore, visualisation into the middle ear (ME) is limited; dictated by the translucency of the TM and severity of any effusion present. Deeper middle ear structures such as the round window or stapes footplate are not visible. These optical limitations play a part in the poor diagnostic accuracy of standard otoscopy for common conditions such as otitis media.<sup>1</sup> Acute otitis media (AOM) is the most common reason for antibiotic prescription in children in the United States<sup>2</sup> accounting for up to \$2.8 billion in medical costs a year.<sup>3</sup> Diagnosis is made through otoscopic examination findings of TM redness and bulge with pneumatic otoscopy used to confirm reduced TM mobility. Yet, AOM may be clinically challenging to differentiate from otitis media with effusion (OME), a condition where ME fluid is present but with no bacterial infection, as children with OME typically present asymptomatic. Standard otoscopy for OME provides low sensitivity (74%-87%) and specificity (60%-74%)<sup>4-6</sup> with some estimates suggesting OME is misdiagnosed as AOM in up to 30% of children.<sup>1</sup> Under-diagnosis of

AOM may lead to lasting hearing morbidity in children, while over-diagnosis may lead to over-prescription and antibiotic resistance.<sup>6,7</sup> While adjunct diagnostic tools such as pneumatic otoscopy and tympanometry may provide higher sensitivity and specificity (70-90%),<sup>4-6</sup> they are still recommended to be used in conjunction with otoscopy. In other otological pathology such as conductive hearing loss (CHL), identification of the cause is achieved through audiometric testing, as there is currently no clinical tool capable of directly visualising the location of ossicular chain pathology. CT and MRI are used for recurrent or complicated ME pathology and surgical planning. CT is well suited for bony abnormalities and other causes of ME opacification, however, it has poor soft tissue differentiation and has associated radiation exposure. MRI normally excels in soft tissue differentiation, but lacks the resolution to clearly visualise the thin TM, and imaging is compromised by metal implants and poor patient tolerance. An unmet need exists for a diagnostic tool that can provide real-time, high-resolution imaging of the TM and ME with functional information for the clinician to differentiate otitis media types, identify causes of CHL and assist ME surgical planning.

Optical coherence tomography (OCT) is an established non-invasive, non-contact imaging modality that allows rapid sub-surface visualisation of tissue microstructure at high resolution. OCT has several advantages over the current imaging standards. The high resolution of OCT (5-15 $\mu$ m) enables characterisation of the thin, low-contrast, soft-tissue TM and complex ME structures that CT (400 $\mu$ m), MRI (300 $\mu$ m) or ultrasound (150 $\mu$ m at 10MHz) cannot readily resolve. OCT is readily adapted to handheld probes or surgical

microscopes allowing real-time, in-vivo imaging without the radiation exposure of CT or the cost of MRI. OCT does not require a transduction medium, as with ultrasound<sup>8</sup>, making structures in the air-filled ME cavity visible.

In this review, we focus on the current state-of-the-art in OCT for TM and ME imaging, and the potential it has to improve the quality of otological diagnostics and surgical planning. Next, the challenges of clinical imaging with OCT in otology are discussed and we explore how they are being overcome. We conclude discussing what steps are required to achieve a future where OCT is in common clinical use in otology, learning from the journey OCT in ophthalmology took to reach widespread clinical acceptance.

## Methods

A literature search of the PubMed, Embase, Google Scholar, Scopus and Web of Science databases was performed to identify all publications from January 1966 to January 2018 using OCT or any other imaging modality to capture TM and ME morphology and according to PRISMA guidelines (Figure 1). Using the key terms “tympenic membrane OR middle ear” and “imaging” returned 515 reports. A separate search with the terms “tympenic membrane OR middle ear” and “optical coherence tomography” yielded 19 reports. The combined 532 abstracts and their reference lists were reviewed with these inclusion criteria: (1) human or animal TM/ME imaging in-vitro, in-vivo, or ex-vivo with OCT, (2) experimental studies discussing new OCT techniques applied to the TM/ME, (3) other non-invasive, non-ionising, portable or handheld TM/ME imaging modalities; and exclusion criteria: (1) non-English

language publications, (2) exclusively theoretical studies with no demonstration of OCT or non-OCT techniques in an animal model or human subject. Of the final 36 studies selected, 15 corresponded to exclusively basic research in animals or ex-vivo cadaveric temporal bones, while 21 were human in-vivo TM/ME imaging studies.

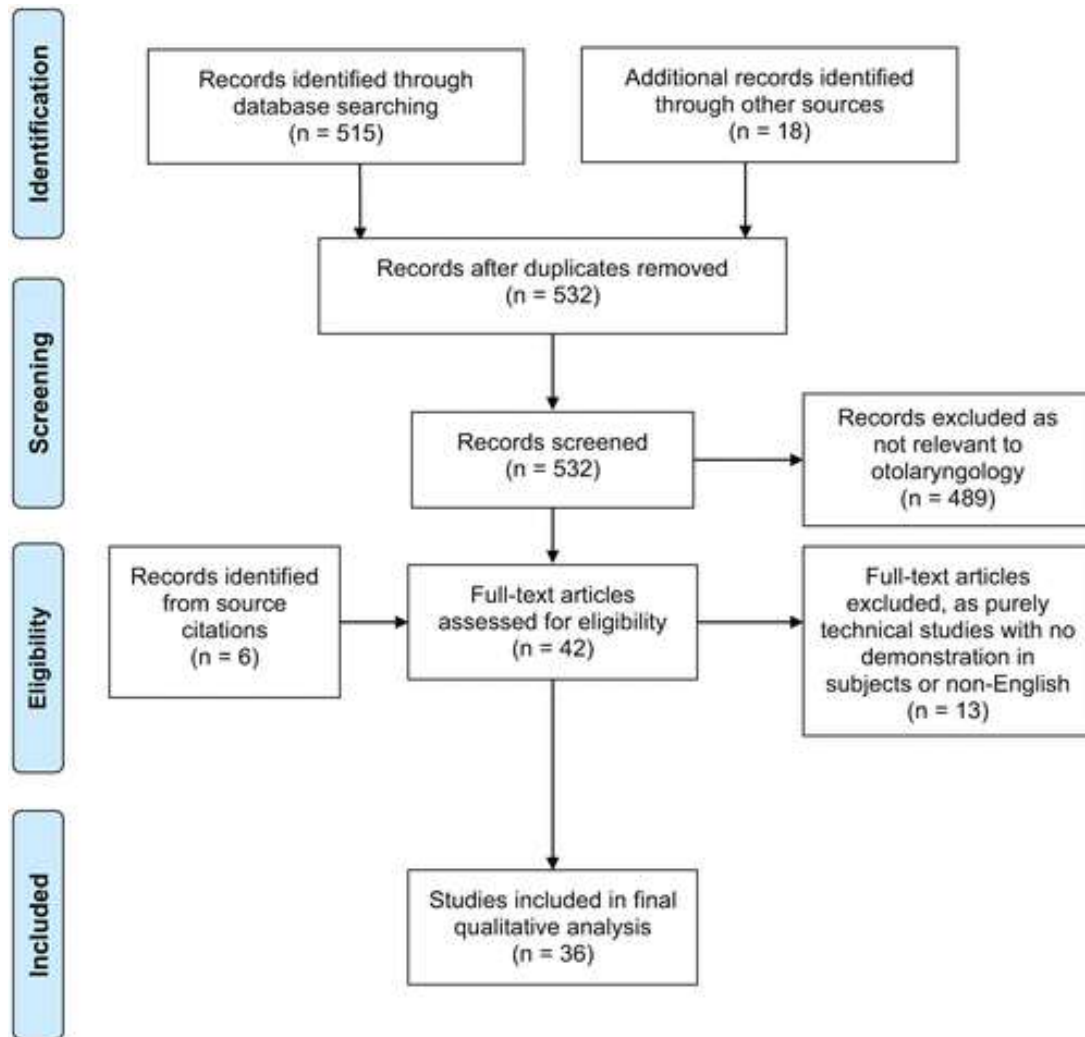


**Figure 1** – Preferred Reporting Items for Systematic Reviews and Meta-Analyses (PRISMA) flowchart summarizing the search results and the application of eligibility criteria.

## Discussion

### OCT working principles, development and clinical application

OCT is conceptually analogous to ultrasound imaging, utilising time-of-flight (time to reach an object and return back) information of light waves to localize tissue structures in depth. Unlike in ultrasound, in which sound wave echoes can be measured directly, OCT measurement is indirect, utilising the principles of low-coherence interferometry.<sup>9-11</sup> OCT systems typically have a resolution of 5-15 $\mu$ m, and are capable of capturing 3D-volumetric data on the order of seconds.<sup>12</sup> However, 3D acquisition of whole volumes at near video rate<sup>13</sup> and 1-2  $\mu$ m resolutions have been demonstrated.<sup>14</sup> The lateral field of view is typically 5-15 mm, and depending on the optical scattering and absorption properties of the tissue, the use of near-infrared light allows OCT to achieve 1-3 mm of depth penetration.

OCT was first demonstrated in 1991 where it was used to capture cross-sectional images of the retina and coronary artery in-vitro<sup>15</sup> and early support from industry led to the first commercial ophthalmic OCT system released in 1996 by Carl Zeiss Meditec Inc.<sup>11,16</sup> However, clinical adoption was slow and proved difficult; limited funding and clinical interest almost halted its development in 2001.<sup>17</sup> It required significant perseverance from researchers and clinicians with limited research funding producing a large volume of clinical data to achieve FDA approval of an OCT system by Optovue in 2006,

by which time over 20 million ophthalmic OCT procedures had already been performed worldwide.<sup>17</sup> Presently, OCT is a key diagnostic technology in ophthalmology with over 30 million ophthalmic OCT procedures performed worldwide per year, a utilisation rate comparable to MRI and CT.<sup>17</sup> OCT research continues to be an area of rapid development as demonstrated by the increasing number of publications with the keywords “optical coherence tomography” published per year (Figure 2).

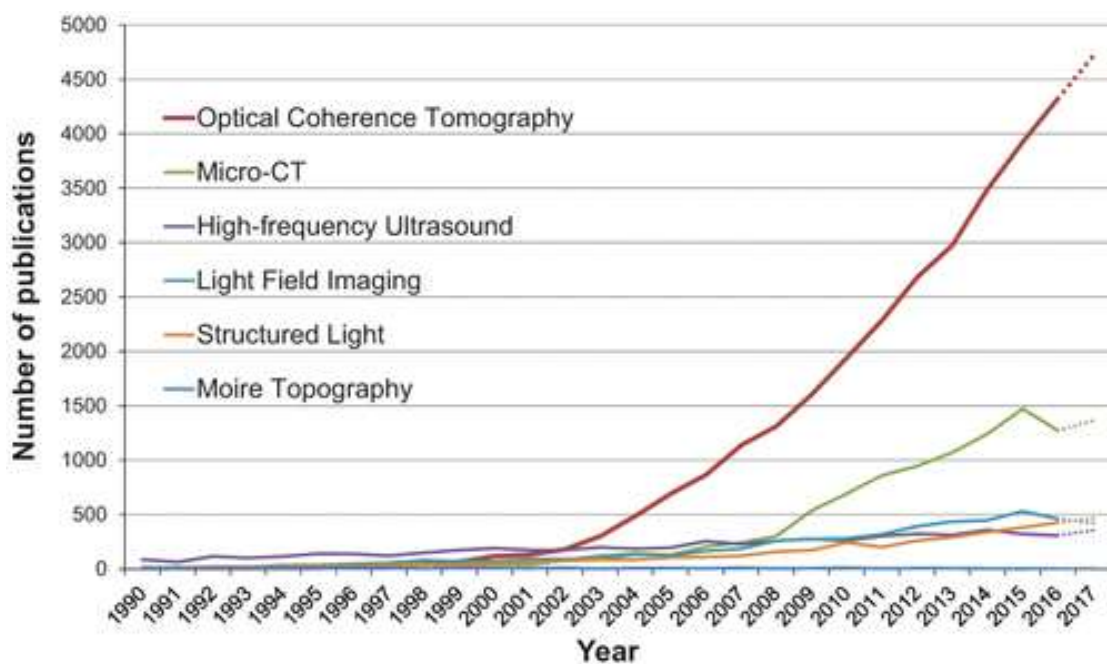


**Figure 2** – Plot of the number of PubMed publications with Optical Coherence Tomography or other imaging modalities as keywords from 1990-2016, showing the rapid development of research interest in OCT. The dashed lines represent data extrapolated for 2017, based on the number of publications as of September 2017.

The feasibility of OCT imaging for the TM and ME was first demonstrated in 2001 (Figure 3a)<sup>18</sup> when normal ME structures were imaged in four ex-vivo temporal bones. The trilaminar nature of the TM could be visualised, as well as the manubrium of the malleus and tensor tympani tendon and the authors

proposed that the higher-resolution, real-time and contactless nature of OCT held potential for “diagnosis and presurgical evaluation of middle ear abnormalities”.<sup>18</sup> However, despite the widespread clinical adoption and commercial success of OCT in ophthalmology, it was another decade before a marked interest developed in OCT technology for TM and ME imaging in otology, where the first in-vivo application was to intraoperatively differentiate cholesteatoma<sup>19</sup> (Figure 3b) from inflamed mucosa and the first portable, handheld TM OCT imaging device was described.<sup>20</sup>

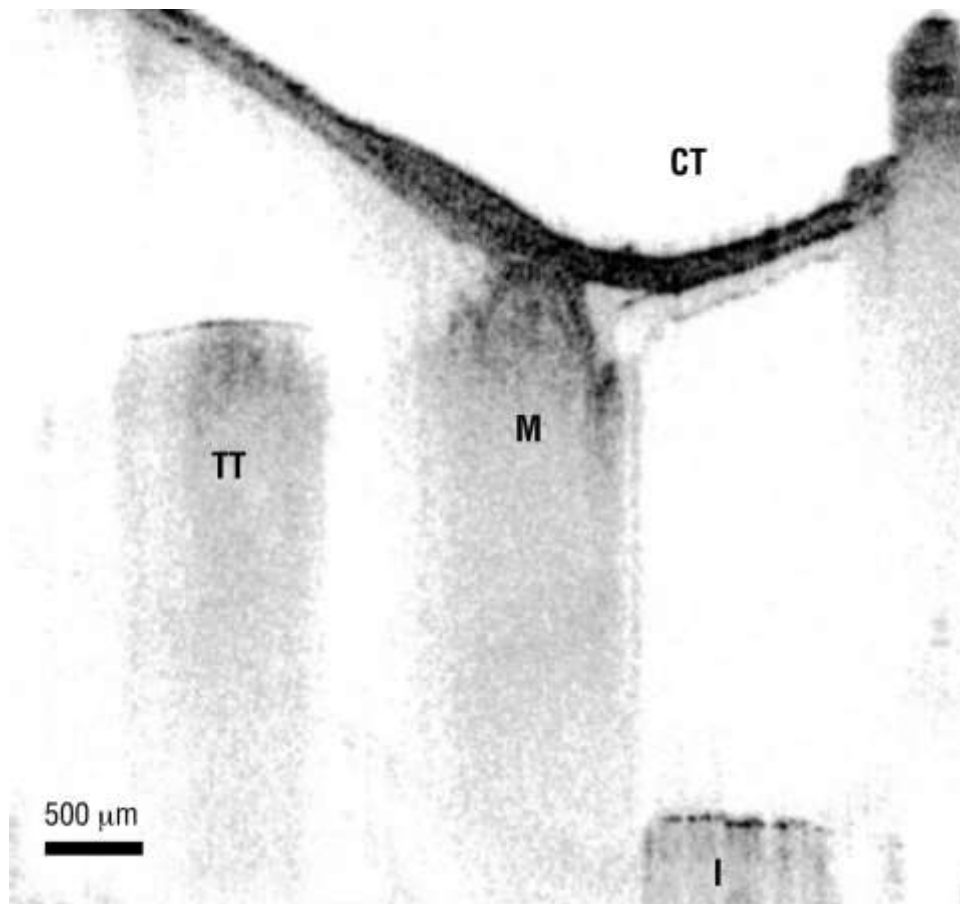


**Figure 3a** – First OCT image of the normal TM and ME, taken ex-vivo through the ear canal of a cadaver temporal bone in 2001, adapted from Pitris et al.<sup>18</sup>

*Figure 3a subheading:* Single arrow – cholesteatoma confirmed by histology, Double arrow – inflamed middle ear mucosa, Dotted white line – demarcating the hyperintense layer due to thick keratin

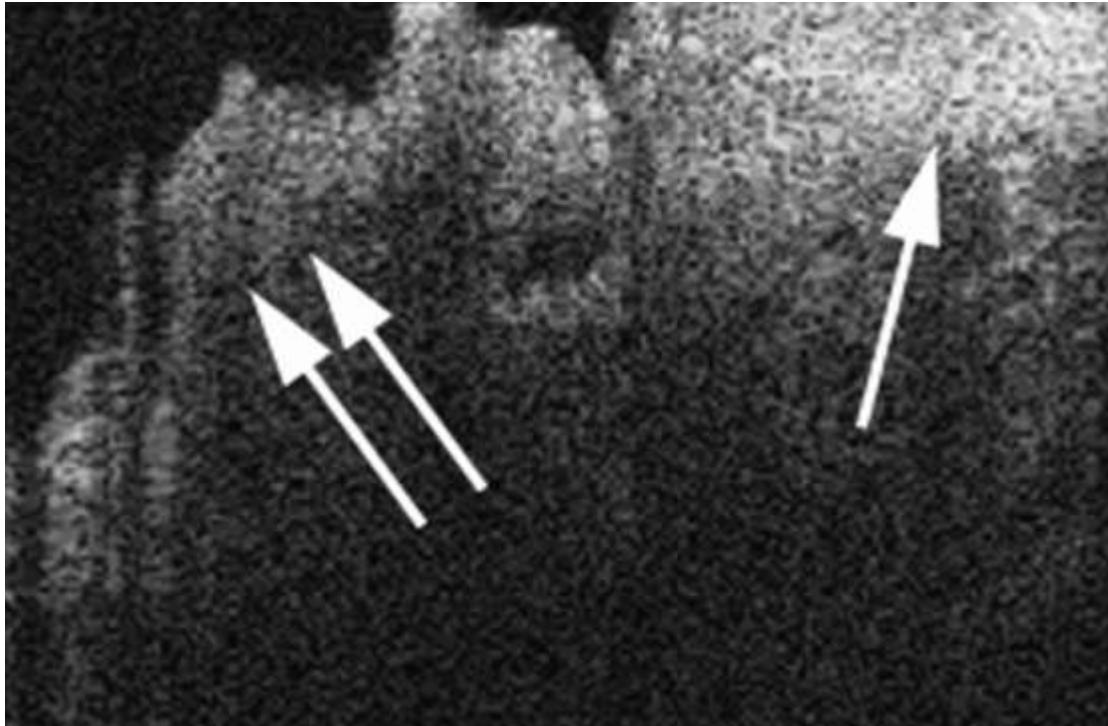


**Figure 3b** – An intraoperative OCT image showing cholesteatoma (single arrow) with its characteristic hyperintensity due to overlying keratin adjacent to inflamed middle ear mucosa (double arrow), adapted from Djalilian et al.<sup>58</sup>

*Figure 3b subheading:* CT – chorda tympani, M – malleus, TT – tensor tympani muscle, I – incus

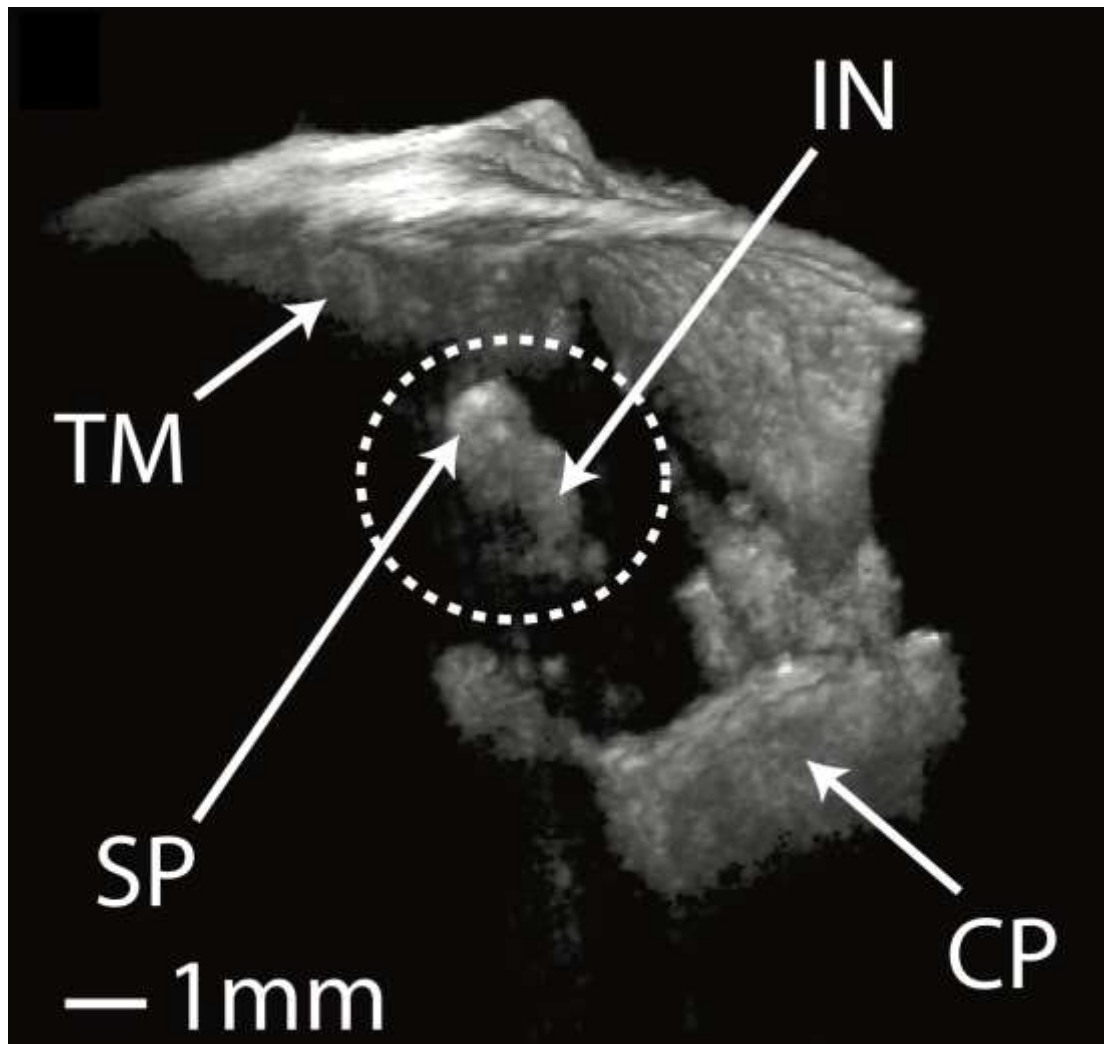


**Figure 3c** – In-vivo 3D OCT volumetric reconstruction of a patient’s ME with a stapes prosthesis (SP) crimped along the long process of the incus (IN). The 3D render allows visualisation of the cochlear promontory (CP) inferiorly and tympanic membrane (TM) superiorly, adapted from MacDougall et al.<sup>46</sup>

In otolaryngology, “optical biopsy”, or non-invasive probe-based OCT characterisation of tissue pathology, promises to reduce tissue trauma, reduce pathology results and patient waiting times and potentially eradicate the need for tissue biopsy altogether.<sup>21</sup> OCT can delineate several pathological lesions such as hyperkeratosis, dysplasia, neoplasia and inflammation; however, the end goal is differentiation between clinically similar

areas (e.g. dysplasia vs. carcinoma-in-situ) rather than simple normal vs. abnormal tissue.<sup>21</sup> OCT has to date focused on examining the laryngeal mucosa for the differentiation of benign and invasive vocal cord cancer, through evaluating basement membrane integrity, epithelium thickness and lamina propria structure.<sup>22,23</sup> Beyond the larynx, OCT has been used to examine the subglottic epithelium changes in prolonged mechanical ventilation in paediatric and neonatal patients.<sup>24</sup> In rhinology, OCT has been used to examine changes to the nasal septum mucosa following septoplasty, different types of rhinitis and decongestant use.<sup>25-27</sup>

## OCT imaging of the tympanic membrane

The recent focus of clinical OCT imaging of the TM (see Table 1 for the last 5 years, see supplemental table 1 for all studies used for this review), has been on improving the diagnosis of OM, where handheld OCT probes (see Figure 4a) have demonstrated the ability to detect presence of biofilm behind the TM, which is suggestive of chronic OM.<sup>28-30</sup> Using OCT-detected biofilm to diagnose chronic OM, one study with 20 patients reported higher diagnostic sensitivity (83% vs. 74%) and specificity (98% vs. 60%) over standard otoscopy.<sup>28</sup> TM thickness is a proposed metric to differentiate between chronic and acute OM, assisting earlier detection and guiding antibiotic management. OCT measures the overall TM thickness, which is the sum of TM the and biofilm layer thickness.<sup>31,32</sup> In 34 paediatric patients, acute OM correlated to a thicker TM, while chronic OM had normal TM thickness but greater biofilm and overall TM thickness – suggesting that the TM tissue returns to relatively normal thickness levels in chronic OM, but the overall TM

**Table 1:** Papers from the last 5 years reporting OCT for TM or ME imaging

Author (Year)	Imaging setting	Sample / number of patients	Ear structure imaged	OCT imaging role / purpose	OCT type	Resolution	
						<i>Trans- verse</i>	<i>Axial</i>
Jang et al. (2013) <sup>51</sup>	Ex-vivo	20 guinea pig chronic TMP model	TM	Evaluate thickness of an experimental TM repair scaffold	SD-OCT	-	8 µm
Chang et al. (2013) <sup>54</sup>	Ex-vivo	3 chinchilla TB	TM + ossicular chain	3D vibrational patterns of TM and ossicular chain in physiological and pathological ear	SD-OCT	25 µm	12 µm
Van der Jeught et al. (2013) <sup>49</sup>	Ex-vivo	6 human TB (5 healthy, 1 with retraction)	TM	Determine the 3D full-field thickness distribution of 5 TM	SD-OCT	<10 µm	<10 µm
Nguyen et al. (2013) <sup>29</sup>	In-vivo (outpatie nt)	6 patients (1 healthy, 5 with chronic OM)	TM	Detection of bacterial biofilm on TM	SD-OCT	-	3.1 µm
Rutledge et al. (2013) <sup>50</sup>	Ex-vivo	1 chinchilla TB + 1 human TB	TM	Determine collagen fibre size and arrangement	SD-OCT	-	-
Burkhardt et al. (2014) <sup>56</sup>	Ex-vivo	1 freshly excised human TM	TM	Doppler OCT for vibration behaviour of 3D TM	SS-OCT	13 µm	9 µm
Guder et al. (2014) <sup>36</sup>	In-vivo (outpatie nt)	47 patients (11 myringitis, 13 retraction, 12 TM-sclerosis, 11 perforation)	TM	Thicker TM in chronic myringitis vs. normal and other TM pathology	SD-OCT	23 µm	10 µm

Pawlowski et al. (2015) <sup>42</sup>	Ex-vivo	1 mouse TB	Middle ear + ossicles	Development of a miniature tunable OCT endoscope	SD-OCT	-	-
Cho et al. (2015) <sup>31</sup>	In-vivo (outpatient)	39 patients with chronic OM + 6 healthy (22 TMs imaged)	TM	Characterisation of TM biofilm and effusion	SD-OCT	10 µm	6 µm
Hubler et al. (2015) <sup>39</sup>	In-vivo (outpatient)	1 patient	TM	TM thickness measurement to detect biofilm	SD-OCT	15 µm	2.4 µm
Monroy et al. (2015) <sup>32</sup>	In-vivo (outpatient)	34 paediatric patients with OM	TM	Thicker TM in acute OM, but normal thickness in chronic OM	SD-OCT	15 µm	4 µm
MacDougall et al. (2016) <sup>46</sup>	Ex-vivo + In-vivo (outpatient)	1 human TB + 1 patient	TM + ossicular chain	Real-time, full-ME 3D scan and trans-TM Doppler vibrography	SS-OCT	<40 µm	<40 µm
Pande et al. (2016) <sup>40</sup>	In-vivo (outpatient)	6 healthy patients (7 TMs imaged)	TM	Mapped full-field TM thickness distribution	LCI	-	-
Park et al. (2016) <sup>55</sup>	Ex-vivo	5 human TB	TM + ossicular chain	Vibration patterns of the TM, ossicles	PS-SD-OCT	15 µm	12 µm
Oh et al. (2016) <sup>89</sup>	In-vivo (animal)	5 mouse + 5 rat	TM + ME	In-vivo imaging of ossicular chain through intact TM	SS-OCT	13 µm	7 µm
Monroy et al. (2017) <sup>34</sup>	Ex-vivo + In-vivo (outpatient)	1 human TB+ 1 patient with ME effusion	TM + middle ear	Measurement of viscosity and diffusion coefficient	SD-OCT	15 µm	4 µm

	nt)			of ME effusion			
Pande et al. (2017) <sup>90</sup>	In-vivo (outpatient)	1 patient	TM	Low-cost probe for TM thickness measurement	LCI	-	5.2 $\mu\text{m}$
Jang et al. (2017) <sup>91</sup>	Ex-vivo	14 rat TMP model	TM	Thickness of an experimental TM repair scaffold	SD-OCT	-	8 $\mu\text{m}$
Park et al. (2017) <sup>64</sup>	In-vivo (outpatient)	1 patient	TM	Clockwise, diagonal-scanning for increased lateral scanning range	SD-OCT	15 $\mu\text{m}$	-
Choi et al. (2017) <sup>92</sup>	Ex-vivo	1 excised dehydrated mouse TM	TM	Vibrational measurements in wide field of view	MFS-OCT	5.04 $\mu\text{m}$	1.8 $\mu\text{m}$
Shelton et al. (2017) <sup>35</sup>	In-vivo (outpatient)	12 patients (16 TMs imaged)	TM	Pneumatic otoscope for TM compliance normal vs. ME effusion	LCI	-	5.6 $\mu\text{m}$
Park et al. (2017) <sup>41</sup>	In-vivo (outpatient)	120 patients (only 85 successful images however)	TM	TM perforation margin thickness, and monitor TM graft healing	LCI	15 $\mu\text{m}$	15 $\mu\text{m}$
Monroy et al. (2017) <sup>33</sup>	In-vivo (outpatient and intraoperative)	25 patients	TM	Confirm biofilm clearance post-tube placement	SD-OCT	15 $\mu\text{m}$	2.4 $\mu\text{m}$

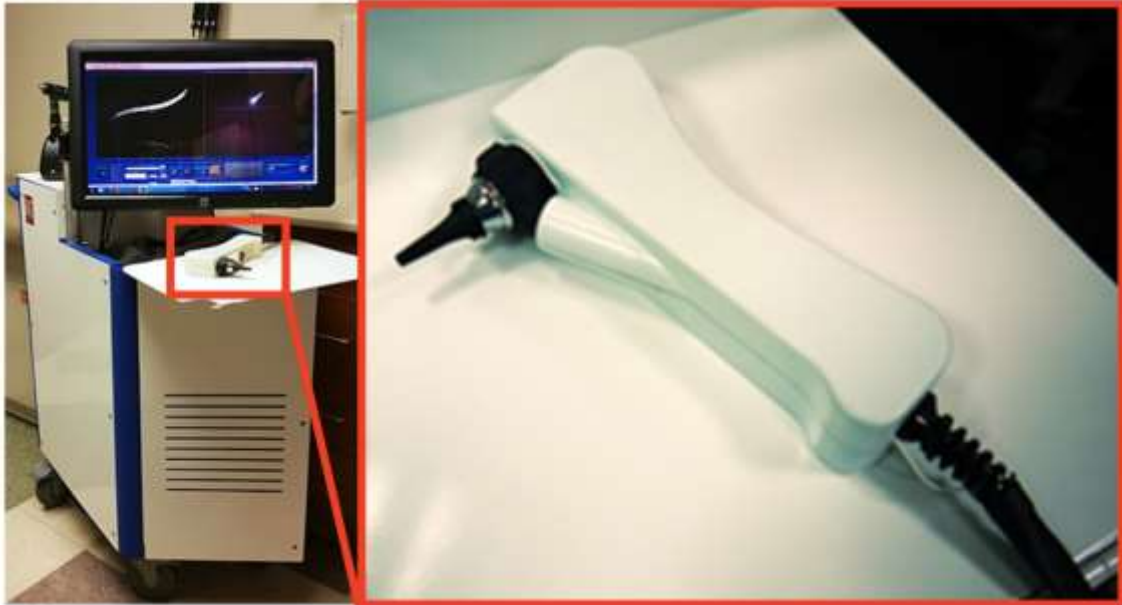


**Figure 4a** – A non-invasive handheld OCT probe developed primarily for the purpose of measuring TM thickness to assess for biofilm presence, and to characterise ME effusion viscosity to differentiate OM types, adapted from Monroy et al.<sup>33</sup>



**Figure 4b** – An OCT system mounted onto a surgical microscope arm, with coupled Doppler vibrography for real-time, whole-ME 3D volume reconstruction and ME diagnostics, adapted from MacDougal et al.<sup>46</sup>

remains thicker due to an increased biofilm layer.<sup>31,32</sup> As a follow-up diagnostic tool, in a recent prospective series of 25 paediatric patients with chronic or recurrent OM undergoing myringotomy and tympanoplasty tube placement, four out of six patients available to 6-month follow-up demonstrated clearance of middle ear biofilm on handheld-OCT imaging, which correlated with clinical findings.<sup>33</sup> For OME, standard and pneumatic otoscopy provides qualitative assessment of TM bulging and effusion. As such, OCT has been proposed as a tool to assess the degree and turbidity of effusion in OME to quantify severity of chronic OM and monitor resolution of infection.<sup>34</sup> Building upon this, by coupling OCT and pneumatic otoscopy into a single device, quantitative assessment of TM compliance as determined by minute deflections of the TM has been achieved, demonstrated in a pilot study of 15 patients (16 imaged ears) where average compliance across 10 healthy ears (6.1 microns/mmHg) was higher and statistically different to 4 ears with OME (1.4 microns/mmHg).<sup>35</sup>

By adapting OCT to the surgical microscope, it has been used to detect microanatomical changes found in the TM layers of patients with chronic myringitis.<sup>36,37</sup> OCT can visualise the loss of the trilaminar TM structure, loss of outer epithelial layer integrity and separation of outer and inner TM layers occurring in chronic myringitis – information not visible with an operating microscope.<sup>36</sup> The high signal intensity of keratin distinguishes it from normal or inflamed ME mucosa (Figure 3b); this may assist the surgeon to detect and remove any residual cholesteatoma buried within mucosal tissue that could be missed using a standard operating microscope.<sup>38</sup> Mapping and tracking the

changes in TM thickness of the entire TM with in-vivo OCT can describe retraction pocket depth and confirm increased thickness of the white, chalky patches in tympanosclerosis.<sup>39,40</sup> Recently, a handheld OCT-based otoscope was used to monitor healing of inserted grafts following tympanoplasty, assessing the interface contiguity between graft and native TM and demonstrating the thinning over time that temporalis fascia grafts undergo during healing.<sup>41</sup> In the same patient series of 120 patients, OCT also provided precise measurements of TM perforation margin thickness (thicker in chronic perforations), matching the oto-endoscopic estimates of margin thickness from three otologists which suggested oto-endoscopy is reliable for perforation margin assessment.<sup>41</sup> For assessment of TM retraction severity however, OCT was superior in differentiating intermediate-staged TM retraction, unlike concurrent oto-endoscopy findings where it was indistinguishable to other severity stages, demonstrating another potential application of OCT as an complementary, objective tool in otology.<sup>41</sup>

## OCT imaging of the middle ear

The opacity and reflectivity of the TM hampers optical imaging into the ME cavity by attenuating the signal and creating shadowing artefacts. As such most OCT clinical imaging of the ME to date has been performed intra-operatively, where the TM has been removed. OCT imaging of the ME has been applied in the form of a 1mm fine endoscope catheter that can be passed through an existing TM perforation to characterise ossicular chain morphology and vibrational characteristics.<sup>42</sup> OCT can be mounted on the articulating arm of a surgical microscope (see Figure 4b) where it has been

used to measure distances for stapes prosthesis implantation, avoiding mechanical measurement which risks breaking the stapes footplate or remaining chain, and allowing confirmation of prosthesis position below the TM and in relation to the long process of the incus at follow up (see Figure 3c), which is hard to assess with otoscopy.<sup>43</sup> Intraoperative OCT has also characterised the morphology of the stapes footplate, identifying sclerotic changes to the elastic suspension of the stapes footplate in patients undergoing stapedectomy for otosclerosis.<sup>44,45</sup> Looking forward, OCT holds greatest value, in its use in combination with other modalities for functional diagnostics, such as with laser Doppler vibrography (see Figure 4b) and acquisition methods, such as phase-sensitive OCT, where it has demonstrated the potential for real-time, in-vivo middle ear diagnostics and vibrometry.<sup>46,47</sup> However, patient motion must be addressed as one study found that in OCT Doppler vibrometry imaging of live patients, motion due to respiration, heartbeat or muscle movement caused motion-artefact several orders of magnitude larger than the physiological TM displacement, degrading image sensitivity.<sup>46</sup>

## OCT imaging as a research tool

OCT is a key research tool in experimental middle ear and hearing research, as researchers can remove the EAC to closer image the TM and to view the medial side of the TM.<sup>48</sup> Using OCT to characterise the thickness distribution of the ex-vivo TM has assisted hearing researchers to create better mathematical and finite element models of middle ear biomechanics and has a role to play in surgical prosthesis and graft modelling.<sup>49,50</sup> As an imaging

tool, OCT has been used as a tool to assess the healing of experimental grafts in mouse models<sup>51</sup> and, in another study, to assess the 'fit' and placement of a film patch (with integrated strain gauge that was used to detect TM movement) on a normal TM.<sup>52</sup> Using high-sensitivity optical microangiography with OCT, 3D volumetric representations of blood flow in the cochlea of mice have been created.<sup>53</sup> Crucial to the study of middle ear biomechanics, OCT has been used to visualise sound-induced TM and ossicular motion at different frequencies and for different pathologies such as stapes fixation and incudo-stapedial disruption with the clinical goal to translate OCT as adjunct to middle ear diagnostics.<sup>54-57</sup>

## The challenges of clinical tympanic membrane and middle ear imaging with OCT

The shape of the external auditory canal (EAC) and position of the TM present a challenge for endoscopic design. OCT requires a clear line-of-sight, which is difficult in the narrow, angled external auditory canal. This is further complicated as imaging the whole surface of the TM and the visually obscured regions of the ME cavity, such as the sinus tympani, is often desired.<sup>58</sup> Presently, visualisation requires a conical ear speculum to retract the tragus and align the conchal cartilage in order to straighten the EAC and often requires the removal of wax. The inferior (43 degrees to the horizontal plane) and medial projection (34 degrees to parasagittal plane) of the TM<sup>59</sup> means that the inferior and anterior quadrants are situated deeper relative to the axis of the EAC, and are thus in a different focal plane if approached directly along the axis of the EAC. OCT is thus required to have a focal depth

and imaging range of 3 to 4 mm for the TM, and 10mm for the ME,<sup>46</sup> which is achievable, but at a significant cost to transverse resolution. While OCT devices do not cause ear canal discomfort through pain or heat, the need for patients to remain completely motionless in order to reduce motion artefact, may be challenging, particularly in uncooperative young children.

In order to image the ME cavity, the imaging beam must first pass through the TM, backscatter off a middle ear structure and pass back through the TM to the detector – a challenge worsened in cases of pathological thickening or calcification of the TM.<sup>19,60</sup> As light needs to pass through the TM twice, up to 89% of original incident photons are scattered resulting in a source signal loss of up to 19dB as found in ex-vivo analysis of normal TM.<sup>60</sup> In addition, the reflectivity of the TM can obscure weaker reflections of other middle ear structures, though when compared to signal loss due to scattering, these are considered negligible.<sup>60</sup> Capturing the full volume of the ME through the intact TM is challenging but has been performed in ex-vivo temporal bones<sup>18,55</sup> and live patients.<sup>46</sup> The ME can also be imaged through a perforation with a fine endoscope<sup>42</sup>, or as demonstrated for cochlea imaging, a flexible, thin, catheter-based OCT.<sup>61</sup> However, the requirement for myringotomy to place a catheter may prove too invasive for routine diagnostic use and hence a non-invasive approach is still preferred.

Ideally, an OCT imaging device for the TM and ME will have a wide field of view (at least 8mm to capture the entire TM annulus in one view), large depth of focus (to accommodate the tilted TM), adequate working distance (to avoid

accidental contact with TM), be forward-facing (to assure en-face TM imaging), thin or flexible and endoscopic (to navigate past the narrow EAC isthmus), and rapidly-scanning (to increase patient comfort and reduce the impact of hand motion tremors). However, this is challenging as increasing the depth of focus or increasing the working distance to improve the field of view compromises transverse resolution, and unintentional probe tip movement caused by the patient or operator introduces motion artefact.<sup>62</sup> One approach to overcoming the narrow field of view afforded by the tight ear canal has been to build a composite image of the full surface of TM from various OCT images taken with the ear specula, otoscope and patient's head in different positions.<sup>40</sup>

Lastly, an attractive feature of OCT is the ability to rapidly visualise detail in 3D. Most demonstrations of OCT in otology to date have been one or two-dimensional due to the challenge of motion artefact and limited penetration depth into the ME. It is also challenging to present the 3D volumetric reconstruction OCT data as a live view, as it requires rapid computing power. However, real-time 3D OCT has recently been demonstrated through a system with orthogonal galvanometer mirror scanners mounted on a microscope arm (Figure 4b).<sup>46</sup> This system was the first to demonstrate the ability to capture the entire ME volume of a live patient, at a distance, and excitingly with the incorporation of laser Doppler vibrography. This is a significant step in translating OCT into a ME imaging and functional diagnostic tool for CHL, as it which will allow the live, dynamic assessment of ossicular and TM vibrational patterns in response to sound.<sup>46</sup> Another group achieved

3D visualisation through a wide-field, diagonal-scanning handheld device which overcame motion artefact by crossing over the same location with each scan.<sup>63</sup>

## Other imaging modalities of the tympanic membrane and middle ear

Advanced imaging tools are likely to play an important role in surgical planning of TM and ME surgery by measuring the size and shape of biomaterials used in reconstruction. The need for this information has been driven with the advent of 3D biomaterial printing.<sup>64</sup> Although it has been demonstrated that OCT technology can provide topographical data, advances in other imaging modalities may also provide solutions. Historically, endoscopic photography to achieve 'entire' TM images was first performed in 1967<sup>65</sup> and later fluorescein angiography via endoscopy was used to visualise TM microvasculature and demonstrate temporalis fascia graft revascularisation 2-4 weeks post-tympanoplasty.<sup>66</sup> Structured light imaging is a 3D scanning technique where patterned light (often vertical bars or grids) is projected upon an object and, depending on how these patterns deform about the surface, its depth and surface topography can be recorded.<sup>67</sup> When adapted into a handheld otoscope,<sup>68</sup> or into a surgical binocular microscope,<sup>67,69</sup> structured light is an effective and low-cost approach to acquiring the 3D surface topography of the lateral TM. Another older, low-cost technique used to map the TM surface is Moire topography, an established profilometry technique that creates contour maps from the overlapping interference patterns of coherent light from two sources.<sup>70,71</sup> Surface

topography has also been captured through a light field otoscope based upon a plenoptic camera (Figure 5), an imaging technology that positions an array of microlenses in front of a conventional image sensor to detect the direction and intensity, compared to solely intensity in a conventional camera, of light rays.<sup>72,73</sup> More rudimentary, the lateral surface of the TM can be reproduced by 3D scanning with photogrammetry of cast impressions of the TM and deep ear canal; however, this is a more invasive approach compared to non-contact imaging.<sup>74-76</sup>

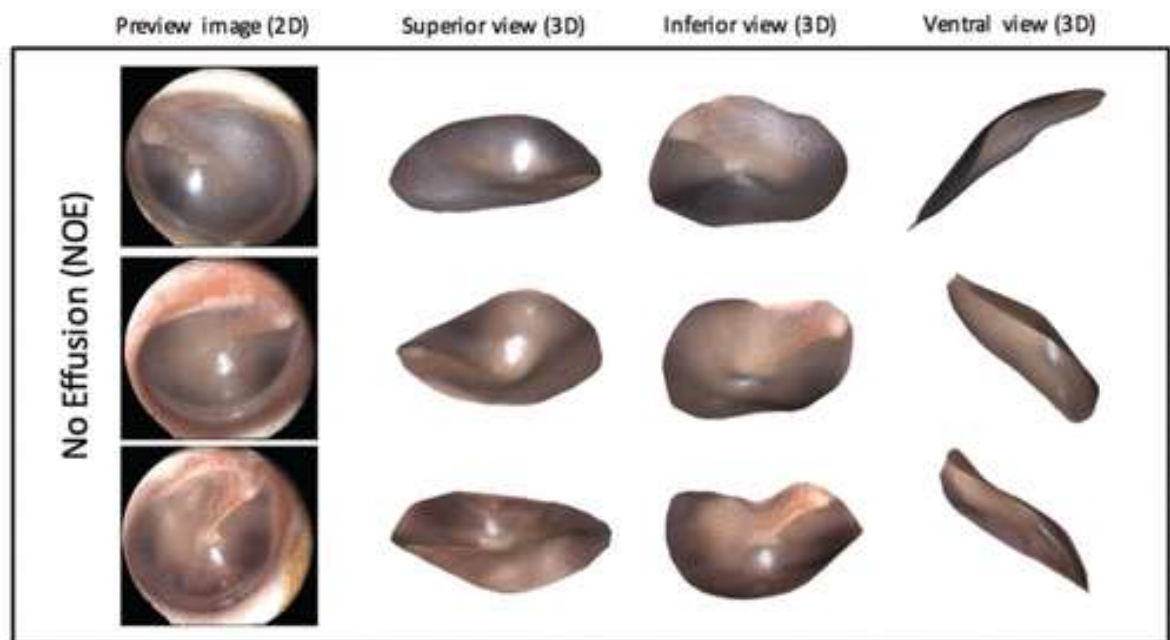


**Figure 5** – Lateral surface of the TM as reconstructed from light field imaging, adapted from Bedard et al.<sup>73</sup>

Accurate modelling of the TM shape is crucial to middle ear biomechanics and finite element modelling.<sup>77</sup> Confocal laser microscopy has been used to create a thickness distribution map in cat TM and to demonstrate the extent of thickness variability between human TM samples.<sup>78,79</sup> Micro-computed tomography is a widely used high resolution imaging tool for finite element

modelling for the middle ear bony structures and cochlear hydrodynamics, and recent use of iodine potassium iodide as a contrast agent increased resolution to sufficiently visualise the thin TM.<sup>80-83</sup> However, micro-CT is not yet clinically ready for patients or larger sized objects. Lastly, high-frequency ultrasonography has demonstrated potential utility in ex-vivo human cadaver TM as a middle ear diagnostic and monitoring tool through real-time vibrometry, though disadvantaged to OCT by its need for saline as an imaging medium.<sup>8</sup>

## Implications for practice

In its current state, OCT for clinical imaging in otology is still far from reaching broad clinical use. In some respects it offers significant value over existing imaging modalities (CT, MRI and micro-otoscopy) but many pathological conditions of the TM and ME do not require diagnostic imaging beyond micro-otoscopy. At its inception, retinal OCT provided an image that could not be achieved with any other technique and yet it still required 5-10 years to fully reach clinical use. For otology, while CT and MRI do not provide the high resolution of OCT, they can still provide imaging sufficient for the accurate radiological diagnosis of causes of ME opacification including cholesteatoma, glomus tympanicum, middle ear schwannoma, congenital malformations or chronic ME inflammation.<sup>84</sup> OCT has provided some detailed pictures and functional information such as biofilm presence, TM thickness and ossicular chain vibration, but the data provided will hold limited clinical value until validation in larger patient trials.

Yet, the future of OCT for otology remains bright. In the future, OCT can play a large role in middle ear infection diagnosis and management. OCT can detect and quantify ME effusions better than regular otoscopy allows, which will provide earlier diagnosis and an indication of severity at first diagnosis. A research OCT system costs approximately US\$50,000-100,000, and a clinical OCT device for otology will likely cost similar to ophthalmic OCT (US\$300,000). OCT devices are significantly cheaper than MRI (US\$1-3M) and CT (US\$1-2M) scanners, however, they are several times more expensive than commonplace clinical tools such as an outpatient microscope (US\$5,000-10,000), tympanometer (US\$2,000-4,000) or otoscope (US\$100-200). As the drive for lower-cost OCT continues, a price-point may be reached where it can be integrated and potentially replace the standard otoscope. Smaller OCT systems will assist clinical translation; OCT 'on-a-chip' aims to miniaturise OCT to the size of a coin by implementing optical components within integrated silicon photonic chips and has reached proof-of-concept.<sup>85</sup> OCT elastography and vibrometry will develop as tools to measure effusion viscosity, which may be used to determine the pathogenesis of OM. Biofilm clearance may be used as a metric of antibiotic responsiveness or success of tympanoplasty tube placement. Specific otopathogenic bacterial species may be identified through Raman spectroscopy allowing directed antibiotic therapy.<sup>86</sup> For hearing diagnostics, OCT vibrography will assist in identifying causes of CHL within the TM and ossicular chain. For surgical follow-up, the high resolution of OCT will allow the monitoring of tympanoplasty graft healing and integration at the microscopic level.

To achieve this future, superior whole-field, real-time 3D imaging with adequate axial resolution to image into the ME will be required. Powerful imaging technology, as summarised in Table 2, continues to develop at a rapid pace. Multi-parameter imaging such as OCT with vibrometry or elastography in a portable form factor will herald a new era in otological diagnostic and monitoring imaging. To make OCT imaging data relevant to clinicians, clinical practice guidelines for otitis media will require changes to reflect the role of biofilm presence and OCT-based diagnosis.<sup>87</sup> Further longitudinal studies in geographically-varied populations and age groups are required to validate the role of OCT-identified ME biofilm.<sup>33</sup> For ME imaging, increasing the field of view and addressing signal attenuation and artefact production from the TM with faster imaging speed will be key for expanding the role of OCT in the middle ear and potentially inner ear. A database of normal and diseased TM topography and ME imaging may aid machine-assisted diagnosis.<sup>88</sup>

Lessons may be learnt from the life cycle and lengthy road to clinical acceptance that OCT took in ophthalmology. OCT for otology finds itself in a similar position to OCT for ophthalmology at its early inception more than two decades ago, with various publications demonstrating proof of concept for clinical application but yet to find clinical acceptance (Figure 6). While technological advancements increased OCT imaging speeds, the tipping point in OCT for ophthalmology (as later reflected upon by the inventing group of OCT<sup>17</sup>) was the development of anti-VEGF therapy for exudative age-related macular degeneration (AMD), where OCT played a unique role in identifying

**Table 2:** Summary of TM imaging modality types

<b>Imaging Modality</b>	<b>Resolution</b>	<b>Penetration depth</b>	<b>Measured value</b>	<b>Utility for TM and ME imaging</b>
Optical coherence tomography	5-10 $\mu\text{m}$	1-3 mm	Optical scattering	High-resolution, non-invasive measurement, rapid 3D ME and TM capture
Computed tomography	400 $\mu\text{m}$	N/A	Absorbed ionising radiation	Unable to resolve the thin TM, but excels in bony features
Micro computed tomography	1 $\mu\text{m}$	N/A	Absorbed ionising radiation	Excellent for small objects, not ready for clinical use
High-frequency ultrasound (HFUS)	30-60 $\mu\text{m}$ at 50MHz	10 mm	HFUS waves reflected from deep structures	Lower resolution and requires saline as a conducting medium, but provides greater penetration depth over OCT
Light field imaging	50-60 $\mu\text{m}$	None (surface only)	Direction and intensity of light via lens microarray	Acquire TM surface topography, but a more costly, early technology
Structured light		None (surface only)	Deformation of projected patterned light (vertical bars)	Real-time profilometry for quantitative TM deformation will assist OME, but limited by the reflectivity of TM
Moire Topography		None (surface only)	Overlapping interference patterns of coherent light	An older method to recreate the 3D surface topography of the TM, but is likely inferior in resolution to other modalities
Confocal laser-microscopy	5 $\mu\text{m}$	300-400 $\mu\text{m}$	3D reconstruction optical slices gained from laser imaging	High-resolution imaging, but limited depth of focus requires a flattened TM and is impractical for in-vivo imaging

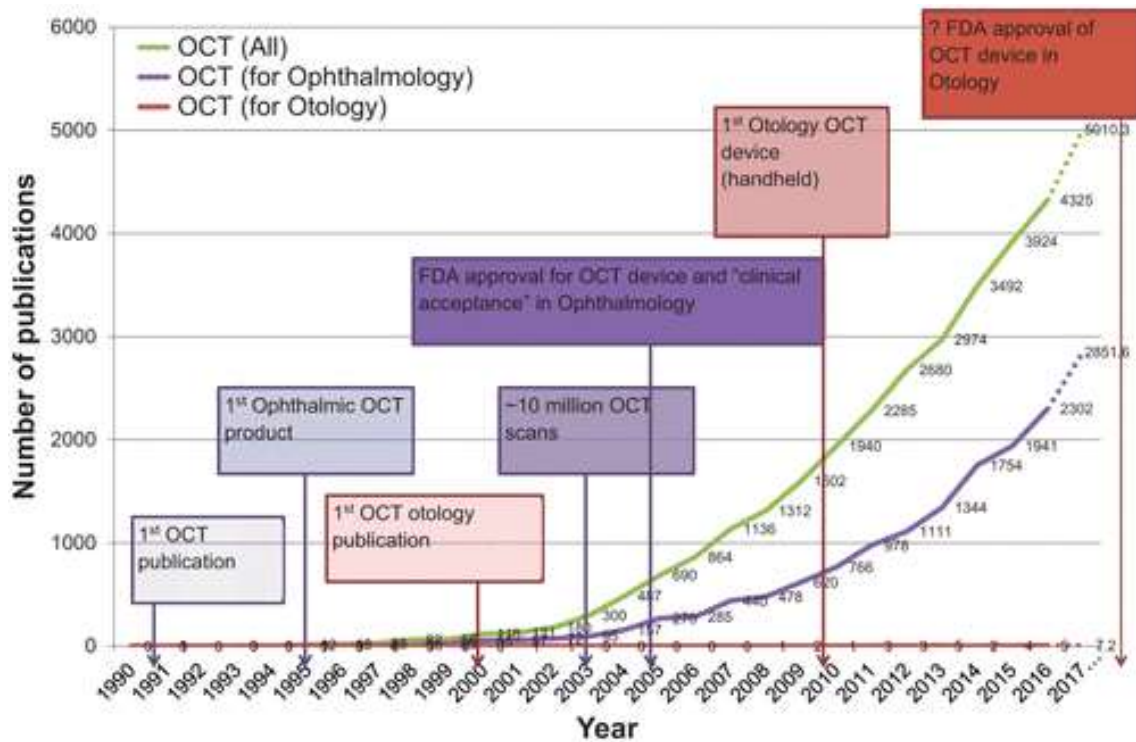


**Figure 6** – Key milestones in the life cycle of OCT in ophthalmology (purple), as compared to OCT in otology (red) as represented by number of publications on PubMed.

treatment response. This gave immediate clinical applicability and linked both diagnosis and therapy. For otology, OCT technology in terms of image resolution and 3D volume acquisition speed surpasses what is clinically needed for diagnostics. However, in the absence of an “AMD tipping point” for otology, clinical acceptance will require focused development to fully utilise the non-invasive, higher resolution and imaging speed advantages of OCT. An ecosystem that allows greater interaction between entrepreneurs, government funding, clinician scientists, researchers, and medical device industries will assist this development.<sup>17</sup> Persistence from research groups to optimise OCT for clinical applications will see to a growing body of supporting evidence for OCT use in otology and commercial interest. The threshold for OCT to enter clinical otology has been set higher by the near-sufficient imaging technology in everyday use. The challenge for future development of

OCT imaging in otology will be to focus on the advantages it provides over existing imaging, and provide clinically relevant information to clinicians beyond that from CT or MRI.

## Conclusion

As OCT continues to develop as a powerful clinical and experimental imaging modality, the price, user-friendliness and clinical usefulness of handheld devices must be considered. Otitis media diagnostics and ossicular chain assessment are key areas where OCT may demonstrate benefit in, particularly through non-invasive identification of specific otopathogens in biofilm and with integration with other parameters such as vibrography and elastography for CHL. OCT for otology still requires significant focused development to reach common clinical use. The barriers of signal attenuation and OCT optics are being addressed in order to image beyond the intact TM with OCT. Moving forward, larger clinical trials focused on the long-term outcomes of OCT-based diagnoses are required to push forth the role of OCT in otology.

## References

1. Blomgren K, Pitkaranta A. Current challenges in diagnosis of acute otitis media. *Int J Pediatr Otorhinolaryngol*. 2005;69(3):295-299.
2. Lieberthal AS, Carroll AE, Chonmaitree T, et al. The diagnosis and management of acute otitis media. *Pediatrics*. 2013;131(3):e964.

3. Ahmed S, Shapiro NL, Bhattacharyya N. Incremental health care utilization and costs for acute otitis media in children. *Laryngoscope*. 2014;124(1):301-305.
4. Kaleida PH, Stool SE. Assessment of otoscopists' accuracy regarding middle-ear effusion: Otosopic validation. *Am J Dis Child*. 1992;146(4):433-435.
5. Lee D-H, Yeo S-W. Clinical diagnostic accuracy of otitis media with effusion in children, and significance of myringotomy: diagnostic or therapeutic? *J Korean Med Sci*. 2004;19(5):739-743.
6. Harris PK, Hutchinson KM, Moravec J. The use of tympanometry and pneumatic otoscopy for predicting middle ear disease. *Am J Audiol*. 2005;14(1):3-13.
7. Pichichero ME, Poole MD. Assessing diagnostic accuracy and tympanocentesis skills in the management of otitis media. *Arch Pediatr Adolesc Med*. 2001;155(10):1137-1142.
8. Landry TG, Rainsbury JW, Adamson RB, Bance ML, Brown JA. Real-time imaging of in-vitro human middle ear using high frequency ultrasound. *Hear Res*. 2015;326:1-7.
9. Boppart SA. Optical coherence tomography: technology and applications for neuroimaging. *Psychophysiology*. 2003;40(4):529-541.
10. Adhi M, Duker JS. Optical coherence tomography – current and future applications. *Curr Opin Ophthalmol*. 2013;24(3):213-221.
11. Rubinstein M, Schalch P, Di Silvio M, Betancourt MA, Wong BJ. Optical coherence tomography applications in otolaryngology. *Acta Otolaryngol*. 2009;60(5):357-363.
12. Drexler W, Fujimoto JG. *Optical Coherence Tomography: Technology and Applications*. 2nd ed: Springer; 2015.

13. Wieser W, Draxinger W, Klein T, Karpf S, Pfeiffer T, Huber R. High definition live 3D-OCT in vivo: design and evaluation of a 4D OCT engine with 1 GVoxel/s. *Biomed Opt Express*. 2014;5(9):2963-2977.
14. Wojtkowski M, Srinivasan VJ, Ko TH, Fujimoto JG, Kowalczyk A, Duker JS. Ultrahigh-resolution, high-speed, Fourier domain optical coherence tomography and methods for dispersion compensation. *Opt Express*. 2004;12(11):2404-2422.
15. Huang D, Swanson EA, Lin CP, et al. Optical coherence tomography. *Science*. 1991;254(5035):1178-1181.
16. Zysk AM, Nguyen FT, Oldenburg AL, Marks DL, Boppart SA. Optical coherence tomography: a review of clinical development from bench to bedside. *J Biomed Opt*. 2007;12(5):051403.
17. Fujimoto J, Swanson E. The development, commercialization, and impact of optical coherence tomography. *Invest Ophthalmol Vis Sci*. 2016;57(9):OCT1-OCT13.
18. Pitris C, Saunders KT, Fujimoto JG, Brezinski ME. High-resolution imaging of the middle ear with optical coherence tomography: a feasibility study. *Arch Otolaryngol Head Neck Surg*. 2001;127(6):637-642.
19. Djalilian HR, Ridgway J, Tam M, Sepehr A, Chen Z, Wong BJ. Imaging the human tympanic membrane using optical coherence tomography in vivo. *Otol Neurotol*. 2008;29(8):1091-1094.
20. Jung W, Kim J, Jeon M, Chaney EJ, Stewart CN, Boppart SA. Handheld optical coherence tomography scanner for primary care diagnostics. *IEEE Trans Biomed Eng*. 2011;58(3):741-744.
21. Jerjes W, Hopper C. Optical diagnostics: Introduction. In: Wong BJF, Ilgner J, eds. *Biomedical Optics in Otorhinolaryngology: Head and Neck Surgery*. New York, NY: Springer New York; 2016:427-430.

22. Rubinstein M, Fine EL, Sepehr A, et al. Optical Coherence Tomography of the Larynx Using the Niris System. *J Otolaryngol Head Neck Surg*. 2010;39(2):150-156.
23. Cernat R, Tatla TS, Pang J, et al. Dual instrument for in vivo and ex vivo OCT imaging in an ENT department. *Biomed Opt Express*. 2012;3(12):3346-3356.
24. Ridgway JM, Su J, Wright R, et al. Optical coherence tomography of the newborn airway. *Ann Otol Rhinol Laryngol*. 2008;117(5):327-334.
25. Ovchinnikov Y, Sobol E, Svistushkin V, Shekhter A, Bagratashvili V, Sviridov A. Laser septochondrocorrection. *Arch Facial Plast Surg*. 2002;4(3):180-185.
26. Meller A, Shakhova M, Rilkin Y, Novozhilov A, Kirillin M, Shakhov A. Optical coherence tomography in diagnosing inflammatory diseases of ENT. *Photonics Lasers Med*. Vol 3 2014:323.
27. Mahmood U, Ridgway J, Jackson R, et al. In vivo optical coherence tomography of the nasal mucosa. *Am J Rhinol*. 2006;20(2):155-159.
28. Nguyen CT, Jung W, Kim J, et al. Noninvasive in vivo optical detection of biofilm in the human middle ear. *Proc Natl Acad Sci U S A*. 2012;109(24):9529-9534.
29. Nguyen CT, Robinson SR, Jung W, Novak MA, Boppart SA, Allen JB. Investigation of bacterial biofilm in the human middle ear using optical coherence tomography and acoustic measurements. *Hear Res*. 2013;301:193-200.
30. Nguyen CT, Tu H, Chaney EJ, Stewart CN, Boppart SA. Non-invasive optical interferometry for the assessment of biofilm growth in the middle ear. *Biomed Opt Express*. 2010;1(4):1104-1116.
31. Cho NH, Lee SH, Jung W, Jang JH, Kim J. Optical coherence tomography for the diagnosis and evaluation of human otitis media. *J Korean Med Sci*. 2015;30(3):328-335.

32. Monroy GL, Shelton RL, Nolan RM, et al. Noninvasive depth-resolved optical measurements of the tympanic membrane and middle ear for differentiating otitis media. *Laryngoscope*. 2015;125(8):E276-282.
33. Monroy GL, Pande P, Nolan RM, et al. Noninvasive in vivo optical coherence tomography tracking of chronic otitis media in pediatric subjects after surgical intervention. *J Biomed Opt*. 2017;22(12):1-11.
34. Monroy GL, Pande P, Shelton RL, et al. Non-invasive optical assessment of viscosity of middle ear effusions in otitis media. *J Biophotonics*. 2017;10(3):394-403.
35. Shelton RL, Nolan RM, Monroy GL, et al. Quantitative pneumatic otoscopy using a light-based ranging technique. *J Assoc Res Otolaryngol*. 2017;18(4):555-568.
36. Guder E, Lankenau E, Fleischhauer F, et al. Microanatomy of the tympanic membrane in chronic myringitis obtained with optical coherence tomography. *Eur Arch Otorhinolaryngol*. 2015;272(11):3217-3223.
37. Lankenau Eva M, Krug M, Oelckers S, Schrage N, Just T, Hüttmann G. iOCT with surgical microscopes: a new imaging during microsurgery. *Adv Opt Tech*. 2013;2(3):233.
38. Kumar S, Acharya A, Hadjihannas E, Panagamuwa C, McDermott AL. Pediatric myringoplasty: definition of "success" and factors affecting outcome. *Otol Neurotol*. 2010;31(9):1417-1420.
39. Hubler Z, Shemonski ND, Shelton RL, Monroy GL, Nolan RM, Boppart SA. Real-time automated thickness measurement of the in vivo human tympanic membrane using optical coherence tomography. *Quant Imaging Med Surg*. 2015;5(1):69-77.
40. Pande P, Shelton RL, Monroy GL, Nolan RM, Boppart SA. A mosaicking approach for in vivo thickness mapping of the human tympanic membrane

- using low coherence interferometry. *J Assoc Res Otolaryngol*. 2016;17(5):403-416.
41. Park K, Cho NH, Jeon M, et al. Optical assessment of the in vivo tympanic membrane status using a handheld optical coherence tomography-based otoscope. *Acta Otolaryngol*. 2017:1-8.
  42. Pawlowski ME, Shrestha S, Park J, Applegate BE, Oghalai JS, Tkaczyk TS. Miniature, minimally invasive, tunable endoscope for investigation of the middle ear. *Biomed Opt Express*. 2015;6(6):2246-2257.
  43. Heermann R, Hauger C, Issing PR, Lenarz T. [Application of Optical Coherence Tomography (OCT) in middle ear surgery]. *Laryngorhinotologie*. 2002;81(6):400-405.
  44. Just T, Lankenau Eva M, Huttmann G, Pau HW. Intraoperative application of optical coherence- tomography (OCT) for visualization of the oval window niche. *Laryngorhinotologie*. 2009;88:168-173.
  45. Just T, Lankenau E, Hüttmann G, Pau HW. [Optical coherence tomography in middle ear surgery]. *Hno*. 2009;57(5):421-427.
  46. MacDougall D, Farrell J, Brown J, Bance M, Adamson R. Long-range, wide-field swept-source optical coherence tomography with GPU accelerated digital lock-in Doppler vibrography for real-time, in vivo middle ear diagnostics. *Biomed Opt Express*. 2016;7(11):4621-4635.
  47. Subhash HM, Nguyen-Huynh A, Wang RK, Jacques SL, Choudhury N, Nuttall AL. Feasibility of spectral-domain phase-sensitive optical coherence tomography for middle ear vibrometry. *J Biomed Opt*. 2012;17(6):060505.
  48. Ilgner J, Just T, Farkas C, Lenenbach A, Westhofen M. Optical coherence tomography for the middle and inner ear. In: Wong BJF, Ilgner J, eds. *Biomedical Optics in Otorhinolaryngology: Head and Neck Surgery*. New York, NY: Springer New York; 2016:545-557.

49. Van der Jeught S, Dirckx JJ, Aerts JR, Bradu A, Podoleanu AG, Buytaert JA. Full-field thickness distribution of human tympanic membrane obtained with optical coherence tomography. *J Assoc Res Otolaryngol*. 2013;14(4):483-494.
50. Rutledge C, Thyden M, Furlong C, Rosowski JJ, Cheng JT. Mapping the histology of the human tympanic membrane by spatial domain optical coherence tomography. Paper presented at: MEMS and Nanotechnology, Volume 6: Proceedings of the 2012 Annual Conference on Experimental and Applied Mechanics, 2013; New York, NY.
51. Jang CH, Cho YB, Yeo M, et al. Regeneration of chronic tympanic membrane perforation using 3D collagen with topical umbilical cord serum. *Int J Biol Macromol*. 2013;62:232-240.
52. Just T, Zehlicke T, Specht O, et al. Detection of tympanic membrane movement using film patch with integrated strain gauge, assessed by optical coherence tomography: experimental study. *J Laryngol Otol*. 2011;125(5):467-473.
53. Subhash HM, Davila V, Sun H, et al. Volumetric in vivo imaging of microvascular perfusion within the intact cochlea in mice using ultra-high sensitive optical microangiography. *IEEE Trans Med Imaging*. 2011;30(2):224-230.
54. Chang EW, Cheng JT, Roosli C, Kobler JB, Rosowski JJ, Yun SH. Simultaneous 3D imaging of sound-induced motions of the tympanic membrane and middle ear ossicles. *Hear Res*. 2013;304:49-56.
55. Park J, Cheng JT, Ferguson D, et al. Investigation of middle ear anatomy and function with combined video otoscopy-phase sensitive OCT. *Biomed Opt Express*. 2016;7(2):238-250.

56. Burkhardt A, Kirsten L, Bornitz M, Zahnert T, Koch E. Investigation of the human tympanic membrane oscillation ex vivo by Doppler optical coherence tomography. *J Biophotonics*. 2014;7(6):434-441.
57. Applegate BE, Shelton RL, Gao SS, Oghalai JS. Imaging high-frequency periodic motion in the mouse ear with coherently interleaved optical coherence tomography. *Opt Lett*. 2011;36(23):4716-4718.
58. Djalilian HR, Rubinstein M, Wu EC, et al. Optical coherence tomography of cholesteatoma. *Otol Neurotol*. 2010;31(6):932-935.
59. McManus LJ, Dawes PJD, Stringer MD. The orientation of the tympanic membrane. *Clinical Anatomy*. 2012;25(2):260-262.
60. MacDougall D, Rainsbury J, Brown J, Bance M, Adamson R. Optical coherence tomography system requirements for clinical diagnostic middle ear imaging. *J Biomed Opt*. 2015;20(5):56008.
61. Lin J, Staecker H, Jafri MS. Optical coherence tomography imaging of the inner ear: a feasibility study with implications for cochlear implantation. *Ann Otol Rhinol Laryngol*. 2008;117(5):341-346.
62. Burkhardt A, Walther J, Cimalla P, Mehner M, Koch E. Endoscopic optical coherence tomography device for forward imaging with broad field of view. *J Biomed Opt*. 2012;17(7):071302.
63. Park K, Cho NH, Jang JH, et al. In vivo 3D imaging of the human tympanic membrane using a wide-field diagonal-scanning optical coherence tomography probe. *Appl Opt*. 2017;56(9):D115-D119.
64. Murphy SV, Atala A. 3D bioprinting of tissues and organs. *Nat Biotech*. 2014;32(8):773-785.
65. Mer S, Derbyshire AJ, Brushenko AA, Pontarelli DA. Fiberoptic endoscopes for examining the middle ear. *Archives of Otolaryngology*. 1967;85(4):387-393.

66. Applebaum EL, Deutsch EC. An endoscopic method of tympanic membrane fluorescein angiography. *Ann Otol Rhinol Laryngol.* 1986;95(5 Pt 1):439-443.
67. Van der Jeught S, Dirckx JJJ. Real-time structured light-based otoscopy for quantitative measurement of eardrum deformation. *J Biomed Opt.* 2017;22(1):016008-016008.
68. Das AJ, Estrada JC, Ge Z, Dolcetti S, Chen D, Raskar R. A compact structured light based otoscope for three dimensional imaging of the tympanic membrane. *Proc SPIE Int Soc Opt Eng.* 2015;9303:93031F.
69. Van der Jeught S, Soons JA, Dirckx JJ. Real-time microscopic phase-shifting profilometry. *Appl Opt.* 2015;54(15):4953-4959.
70. Decraemer WF, Dirckx JJ, Funnell WR. Shape and derived geometrical parameters of the adult, human tympanic membrane measured with a phase-shift moire interferometer. *Hear Res.* 1991;51(1):107-121.
71. Dirckx JJ, Decraemer WF. Optoelectronic moire projector for real-time shape and deformation studies of the tympanic membrane. *J Biomed Opt.* 1997;2(2):176-185.
72. Bedard N, Tomic I, Meng L, Berkner K. Light field otoscope. Paper presented at: Imaging and Applied Optics 2014; 2014/07/13, 2014; Seattle, Washington.
73. Bedard N, Shope T, Hoberman A, et al. Light field otoscope design for 3D in vivo imaging of the middle ear. *Biomed Opt Express.* 2017;8(1):260-272.
74. Koyo Y. Morphological studies of the human tympanic membrane. *J Otolaryng Jap.* 1954;57:115-126.
75. Salvinelli F, Maurizi M, Calamita S, D'Alatri L, Capelli A, Carbone A. The external ear and the tympanic membrane a three-dimensional study. *Scand Audiol.* 1991;20(4):253-256.
76. Kirikae I. *The Structure and Function of the Middle Ear.* Tokyo: University of Tokyo Press; 1960.

77. Vollandri G, Di Puccio F, Forte P, Carmignani C. Biomechanics of the tympanic membrane. *J Biomech.* 2011;44(7):1219-1236.
78. Kuypers LC, Decraemer WF, Dirckx JJ, Timmermans JP. Thickness distribution of fresh eardrums of cat obtained with confocal microscopy. *J Assoc Res Otolaryngol.* 2005;6(3):223-233.
79. Kuypers LC, Decraemer WF, Dirckx JJ. Thickness distribution of fresh and preserved human eardrums measured with confocal microscopy. *Otol Neurotol.* 2006;27(2):256-264.
80. Buytaert JAN, Salih WHM, Dierick M, Jacobs P, Dirckx JJJ. Realistic 3D computer model of the gerbil middle ear, featuring accurate morphology of bone and soft tissue structures. *J Assoc Res Otolaryngol.* 2011;12(6):681-696.
81. Tuck-Lee JP, Pinsky PM, Steele CR, Puria S. Finite element modeling of acousto-mechanical coupling in the cat middle ear. *J Acoust Soc Am.* 2008;124(1):348-362.
82. Rohani SA, Ghomashchi S, Umoh J, Holdsworth DW, Agrawal SK, Ladak HM. Iodine potassium iodide improves the contrast-to-noise ratio of micro-computed tomography images of the human middle ear. *J Microsc.* 2016;264(3):334-338.
83. De Paolis A, Watanabe H, Nelson JT, Bikson M, Packer M, Cardoso L. Human cochlear hydrodynamics: A high-resolution  $\mu$ CT-based finite element study. *J Biomech.* 2017;50:209-216.
84. Trojanowska A, Drop A, Trojanowski P, Rosińska-Bogusiewicz K, Klatka J, Bobek-Billewicz B. External and middle ear diseases: radiological diagnosis based on clinical signs and symptoms. *Insights Imaging.* 2012;3(1):33-48.
85. Schneider S, Lauermann M, Dietrich P-I, Weimann C, Freude W, Koos C. Optical coherence tomography system mass-producible on a silicon photonic chip. *Opt Express.* 2016;24(2):1573-1586.

86. Zhao Y, Monroy GL, You S, et al. Rapid diagnosis and differentiation of microbial pathogens in otitis media with a combined Raman spectroscopy and low-coherence interferometry probe: toward in vivo implementation. *J Biomed Opt.* 2016;21(10):107005.
87. Rosenfeld RM, Shin JJ, Schwartz SR, et al. Clinical Practice Guideline: Otitis Media with Effusion (Update). *Otolaryngol Head Neck Surg.* 2016;154(1\_suppl):S1-S41.
88. Myburgh HC, van Zijl WH, Swanepoel D, Hellstrom S, Laurent C. Otitis media diagnosis for developing countries using tympanic membrane image-analysis. *EBioMedicine.* 2016;5:156-160.
89. Oh S-J, Lee I-W, Wang S-G, Kong S-K, Kim H-K, Goh E-K. Extratympanic imaging of middle and inner ear structures of mouse and rat using optical coherence tomography. Paper presented at: Optical Imaging, Therapeutics, and Advanced Technology in Head and Neck Surgery and Otolaryngology, 2017; San Francisco, California.
90. Pande P, Shelton RL, Monroy GL, Nolan RM, Boppart SA. Low-cost hand-held probe for depth-resolved low-coherence interferometry. *Biomed Opt Express.* 2017;8(1):338-348.
91. Jang CH, Ahn S, Lee JW, Lee BH, Lee H, Kim G. Mesenchymal stem cell-laden hybrid scaffold for regenerating subacute tympanic membrane perforation. *Mater Sci Eng C Mater Biol Appl.* 2017;72:456-463.
92. Choi S, Sato K, Ota T, Nin F, Muramatsu S, Hibino H. Multifrequency-swept optical coherence microscopy for highspeed full-field tomographic vibrometry in biological tissues. *Biomed Opt Express.* 2017;8(2):608-621.

**Supplemental Table 1:** All papers (n=36) used in review, reporting the use of OCT for TM or ME imaging

	Author (Year)	Imaging setting	Sample / number of patients	Ear structure imaged	OCT imaging role / purpose	OCT type	Resolution	
							Trans- verse	Axial
1	Pritis et al. (2001)	Ex-vivo	4 human temporal bones	TM	First OCT images of an ex-vivo TM, feasibility study	TD-OCT	10-20 $\mu\text{m}$	15 $\mu\text{m}$
2	Heermann et al. (2002)	In-vivo (intraope rative)	10 patients	Stapes	Intraoperative measurement for stapes	TD-OCT	30 $\mu\text{m}$	12 $\mu\text{m}$
3	Djalilian et al. (2008)	In-vivo (outpatie nt)	10 patients	TM	Characterised the OCT appearance of cholesteatoma	TD-OCT	10 $\mu\text{m}$	7 $\mu\text{m}$
4	Just et al. (2009)	Ex-vivo + In-vivo (intraope rative)	5 human temporal bones + 8 patients	Oval window niche	Intraoperative oval niche and vestibular imaging	SD- OCT	23 $\mu\text{m}$	12 $\mu\text{m}$
5	McGaughe y et al. (2009)	Ex-vivo	1 human stapes bone	Stapes	Evaluation of Femtolas er ablation of stapes	TD-OCT	<50 $\mu\text{m}$	10-20 $\mu\text{m}$
6	Just et al. (2010)	Ex-vivo	1 human stapes bone	Stapes	Evaluation of CO2 laser stapedectomy	SD- OCT	23 $\mu\text{m}$	12 $\mu\text{m}$
7	Subhash et al. (2011)	Ex-vivo	1 Mouse cochlea	Cochlea	Measured cochlear vasculature blood flow velocity	SD- OCT	16 $\mu\text{m}$	13 $\mu\text{m}$
8	Just et al. (2011)	Ex-vivo	3 human temporal bones	TM	Evaluation of strain gauge patch for TM movement	SD-CCT	24 $\mu\text{m}$	12 $\mu\text{m}$

9	Jung et al. (2011)	In-vivo (outpatient)	1 patient	TM	Feasibility of a handheld OCT diagnostic imaging device of clinicians	SD-OCT	14 $\mu\text{m}$	8 $\mu\text{m}$
10	Burkhardt et al. (2012)	Ex-vivo + In-vivo (outpatient)	1 human temporal bone + 1 patient	TM	Development of forward-facing endoscopic OCT device	SD-OCT	7.6 $\mu\text{m}$	28 $\mu\text{m}$
11	Subhash et al. (2012)	Ex-vivo	2 human temporal bones	TM + ossicular chain	Vibrational measurement of ossicles under 500Hz/65dB stimulus	PS- SD-OCT	16 $\mu\text{m}$	13 $\mu\text{m}$
12	Nguyen et al. (2012)	In-vivo (outpatient)	20 patients (16 patients, 4 volunteer)	TM	Detection of bacterial biofilm on TM of patients with chronic OM	SD-OCT and LCI	30 $\mu\text{m}$ (LCI)	4 $\mu\text{m}$ (LCI)
13	Jang et al. (2013)	Ex-vivo	20 guinea pig chronic TM perforation model	TM	Evaluate thickness of an experimental scaffold for TM perforation repair	SD-OCT	-	8 $\mu\text{m}$
14	Chang et al. (2013)	Ex-vivo	3 chinchilla temporal bone	TM + ossicular chain	3D vibrational patterns of TM and ossicular chain in physiological and pathological ear	PS-SD-OCT	25 $\mu\text{m}$	12 $\mu\text{m}$
15	Van der Jeught et al. (2013)	Ex-vivo	6 human temporal bones (5 healthy, 1 with retraction)	TM	Determine the 3D full-field thickness distribution of 5 TM	SD-OCT	<10 $\mu\text{m}$	<10 $\mu\text{m}$

			pocket)					
16	Nguyen et al. (2013)	In-vivo (outpatient)	6 patients (1 healthy, 5 with chronic OM)	TM	Detection of bacterial biofilm on TM	SD-OCT	-	3.1 $\mu\text{m}$
17	Rutledge et al. (2013)	Ex-vivo	1 chinchilla temporal bone + 1 human temporal bone	TM	Determine collagen fibre size, density and arrangement	SD-OCT	-	-
18	Burkhardt et al. (2014)	Ex-vivo	1 freshly excised human TM	TM	Doppler OCT for vibration behaviour of 3D TM	OFDI	13 $\mu\text{m}$	9 $\mu\text{m}$
19	Guder et al. (2014)	In-vivo (outpatient)	47 patients (11 myringitis, 13 retraction, 12 TM-sclerosis, 11 perforation)	TM	Thicker TM in chronic myringitis vs. normal and other TM pathology	SD-OCT	23 $\mu\text{m}$	10 $\mu\text{m}$
20	Pawlowski et al. (2015)	Ex-vivo	1 mouse temporal bone	Middle ear + ossicles	Development of a miniature tunable OCT endoscope	SD-OCT	-	-
21	Cho et al. (2015)	In-vivo (outpatient)	39 patients with chronic OM + 6 healthy (22 TMs imaged)	TM	Characterisation of TM biofilm and effusion	SD-OCT	10 $\mu\text{m}$	6 $\mu\text{m}$
23	Hubler et al. (2015)	In-vivo (outpatient)	1 patient	TM	TM thickness measurement to detect biofilm	SD-OCT	15 $\mu\text{m}$	2.4 $\mu\text{m}$

24	Monroy et al. (2015)	In-vivo (outpatient)	34 paediatric patients with OM	TM	Thicker TM in acute OM, but normal thickness in chronic OM	SD-OCT	15 $\mu\text{m}$	4 $\mu\text{m}$
25	MacDougall et al. (2016)	Ex-vivo + In-vivo (outpatient)	1 human temporal bone + 1 patient	TM + ossicular chain	Real-time, full-ME 3D scan and trans-TM Doppler vibrography	Swept Source-OCT	<40 $\mu\text{m}$	<40 $\mu\text{m}$
26	Pande et al. (2016)	In-vivo (outpatient)	6 healthy patients (7 TMs imaged)	TM	Mapped full-field TM thickness distribution	LCI	-	-
27	Monroy et al. (2016)	Ex-vivo + In-vivo (outpatient)	1 human temporal bone + 1 patient with ME effusion	TM + middle ear	Measurement of viscosity and diffusion coefficient of ME effusion	SD-OCT	15 $\mu\text{m}$	4 $\mu\text{m}$
28	Park et al. (2016)	Ex-vivo	5 human temporal bone	TM + ossicular chain	Vibration patterns the TM and ossicles	SD-OCT	15 $\mu\text{m}$	12 $\mu\text{m}$
29	Oh et al. (2016)	In-vivo (animal)	5 mouse + 5 rat	TM + ME	In-vivo imaging of ossicular chain through intact TM	Swept-source OCT	13 $\mu\text{m}$	7 $\mu\text{m}$
30	Pande et al. (2017)	In-vivo (outpatient)	1 patient	TM	Low-cost probe for TM thickness measurement	LCI	-	5.2 $\mu\text{m}$
31	Jang et al. (2017)	Ex-vivo	14 rat TM perforation model	TM	Thickness of an experimental TM repair scaffold	SD-OCT	-	8 $\mu\text{m}$
32	Park et al. (2017)	In-vivo (outpatient)	1 patient	TM	Clockwise, diagonal-scanning technique for large	SD-OCT	15 $\mu\text{m}$	-

					lateral scanning range			
33	Choi et al. (2017)	Ex-vivo	1 excised dehydrated mouse TM	TM	Vibrational measurements performed over a wide field of view	Multifrequency-swept OCT	5.04 $\mu\text{m}$	1.8 $\mu\text{m}$
34	Shelton et al. (2017)	In-vivo (outpatient)	12 patients (16 TMs imaged)	TM	Pneumatic OCT otoscope for TM compliance normal vs. ME effusion	LCI	-	5.6 $\mu\text{m}$
35	Park et al. (2017)	In-vivo (outpatient)	120 patients (only 85 successful images however)	TM	TM perforation margin thickness, and monitor TM graft healing	LCI	15 $\mu\text{m}$	15 $\mu\text{m}$
36	Monroy et al. (2017)	In-vivo (outpatient and intraoperative)	25 patients	TM	Confirm biofilm clearance post-tube placement	SD-OCT	15 $\mu\text{m}$	2.4 $\mu\text{m}$

TD-OCT = Time-domain OCT, SD-OCT = Spectral-domain OCT, PS-SD OCT = Phase-sensitive spectral-domain OCT, LCI = Low coherence interferometry, OFDI = Optical frequency domain imaging, - = Not reported